Erosion of iron-tungsten model films by deuterium ion irradiation: a benchmark for TRI3DYN

R Stadlmayr[1] , P S Szabo[1] , D Mayer[1], C Cupak[1], W Möller[2] and
F Aumayr[1]

[1] Institute of Applied Physics, TU Wien, Fusion@ÖAW, Wiedner Hauptstraße 8-10, 1040 Vienna, Austria
[2] Institute of Ion Beam Physics and Materials Research, Helmholtz-Zentrum Dresden-Rossendorf, Bautzner Landstraße 400, 01328 Dresden, Germany

E-mail: stadlmayr@iap.tuwien.ac.at

Abstract

The state-of-the-art 3D version of the Monte Carlo sputtering code TRI3DYN was benchmarked with experimental results obtained for iron-tungsten model films. The data which served for comparison concerned: (a) the mass removal rate for Fe-W films (with 1.5 at% W) by prolonged deuterium ion bombardment at 250 eV measured with the quartz crystal microbalance (QCM) technique as a function of ion fluence (up to a total fluence of 4×10^{23} m^{-2}); (b) the change in surface morphology as measured by atomic force microscopy, and; (c) the change in elemental surface compositions as determined by different surface analytical techniques. Our benchmarking studies show that the code TRI3DYN is able to predict the outcome of the experiments, if the information about the initial surface morphology and elemental depth profile measurements of the sample are taken into account. It is not only the dynamical behaviour of the erosion yield with ion fluence that can be reproduced, but also the emerging surface pattern and the observed tungsten enrichment at the structured surface. The code provides a first insight into the reasons for the high influence of surface roughness at the nm scale on the sputtering behaviour of the plasma facing components (PFCs).

Supplementary material for this article is available online

(Some figures may appear in colour only in the online journal)

1. Introduction

The interaction of energetic ions with surfaces causes a number of interesting effects, of which sputtering has a broad field of applications [1–3]. Sputtering by ions of the solar wind plays a major role in space weathering of atmosphere-less planets and moons, and is an important cause of a thin exosphere around these celestial bodies [4]. Ion sputtering is also the basis for a number of technical processes and is used for analysis, cleaning, and smoothing of surfaces, but also for material modification, including ion cutting and milling or thin layer deposition. In magnetically confined nuclear fusion devices, the erosion of plasma-facing components due to sputtering by energetic ion impact from the plasma is of major concern, because this erosion can limit the lifetime of the first wall. The plasma-facing components are exposed to extremely high deuterium fluxes and correspondingly extreme heat loads [5, 6]. A better understanding of sputtering processes in general and the influence of surface morphology changes on the erosion process in particular are therefore desirable. The TU Wien quartz crystal microbalance (QCM) technique has been ideal for the investigation of dynamic changes in the sputtering yield due to ion bombardment under well-defined laboratory conditions [7]. For the interpretation of experimental QCM data, very powerful Monte Carlo (MC) binary collision approximation (BCA) codes, such as TRIDYN [8] or SDTrimSP-3D

Table 1. Elemental composition of the Fe-W films as analysed by RBS and used for TRI3DYN (data taken from [12]).

| thickness [nm]	Fe [at%]	O [at%]	W [at%]	Ar [at%]
670	96.5	1.5	1.5	<1.0

[9] have recently become available. They are capable of modelling dynamic sputtering effects, including the influence of surface morphologies and its changes in full 3D.

In this manuscript we present a detailed comparison between the QCM erosion measurements for Fe-W model films under D ion bombardment and simulations, using the TRI3DYN code. These Fe-W films serve as a model system for W-containing steels such as EUROFER, which could be an attractive and cost-efficient alternative to a full W main chamber first wall in a future fusion device [10, 11].

2. Methods

2.1. Experimental data used for benchmarking

The experimental results used for benchmarking the TRI3DYN code were obtained at TU Wien and were partially presented in [12]. Here we summarize the experimental procedure and main results. Sample preparation and initial analysis was done at IPP Garching, within the EUROfusion work package on plasma-facing components [5, 12]. Fe-W films of 670nm thickness, containing nominally 1.5 at%W, were deposited onto several quartz crystal discs by using magnetron-sputter deposition with multiple targets. The samples were then analysed via Rutherford backscattering spectrometry (RBS) measurements, using a 3 MeV $^4He^+$ beam, confirming the thickness and a W concentration of 1.5 at%. The RBS data, however, also showed an oxygen amount of 1.5 at% (the results are summarized in table 1) [12]. Independently, the elemental composition of the films as a function of depth were determined by sputter-XPS (x-ray photoelectron spectroscopy) measurements performed at the Analytical Instrumentation Centre (AIC) of TU Wien. XPS results obtained with a monochromatized Al K-alpha source (μFocus 350) with a wide-angle lens hemispherical analyser (WAL 150) in combination with a Specs ion source, using 3 keV Ar^{1+} ions for depth profiling, are shown in figure 1. Besides a clear oxide layer in the topmost few nanometers, oxygen as well as some impurities such as C and N were also found in the bulk of the sample. Atomic force microscopy (AFM) images of the virgin samples were taken with a Cypher AFM (Asylum Research) instrument and can be seen in figure 2(a), taken from [12]. The images presented here have a lateral resolution of 200 $\times$ 200 pixels with a scan size of 389 nm $\times$ 389 nm. The surface of the freshly deposited film displays grain-like structures with lengths of about 200 nm and a root-mean-square roughness of 3.2 nm [12]. Sputtering experiments were performed using the QCM technique. A detailed description of this technique can be found in [7]. A sputter ion source provided a D ion beam with 250 eV/D, where the main contribution of the ion beam was
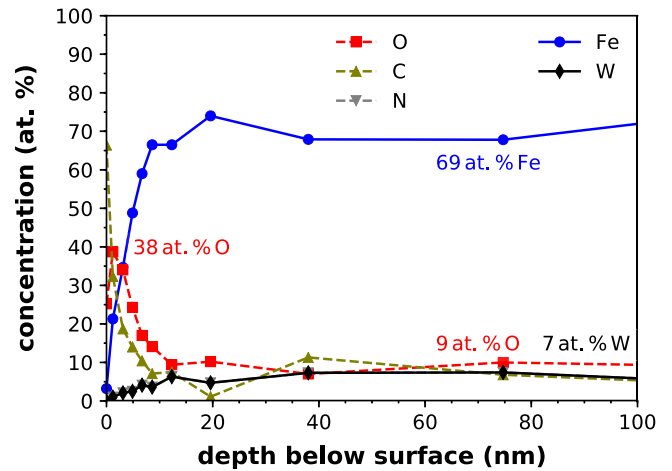

Figure 1. Elemental depth profiles of a virgin Fe-W sample as determined by sputter-XPS and used as input for TRI3DYN. The estimated error of the data points is 10%. An oxide layer at the surface and some light impurities (C, N, O) in the bulk are clearly visible. The bulk material contains up to 7at% W.

D_2^+ in molecular form (94.5%). The ion impact energy is very close to but slightly above the sputtering threshold for W by deuterium projectiles; therefore, the sputtering yield of W is about three orders of magnitude smaller than the yield of Fe. With a deuterium flux of 4×10^{17} m^{-2}s^{-1}, total fluences of up to 4×10^{23} m^{-2} could be applied to the samples. In total, three samples were irradiated under angles of incidence of 0°, 45°, and 60° with respect to the surface normal and at a temperature of 465 K [12]. After irradiation, the surface morphology changes were evaluated by AFM. It should be noted that the QCM technique measures only a change in total mass, which is why the definition of the 'mass removal rate' in units of atomic mass unit per projectile atom is more suitable than the sputtering yield in units of target atoms per projectile atom, and will be used hereinafter.

2.2. Modelling with TRI3DYN

The sputter modelling software TRI3DYN [8] is an enhanced version of TRIDYN [13] and is able to model 3D surfaces. It allows modelling of static as well as dynamic changes of a sputter target. SDTrimSP and TRIDYN are limited in modelling in one dimension (depth). For this, the sputter target is set up in lateral infinite layers, which can be predefined with various elemental concentrations. Only flat sputter targets can be modelled, however. In TRI3DYN this principle has been extended by using small cubic volumes (so-called voxels) with a defined elemental density. These voxels can be stacked on top of each other, so that any 3D structure can be modelled. Expansions of SDTrimSP in 2D as well as 3D are also available, and follow a similar approach [9, 14, 15]. The size of the voxels is a crucial parameter and should be (at least) smaller than the expected collision cascade, to avoid inaccuracies due to discretisation of a real surface. On the other hand, the computing time increases considerably with a large number of voxels, meaning that the lateral extension of the object to be modelled is limited. The code uses the principle of 'pseudoatoms' as
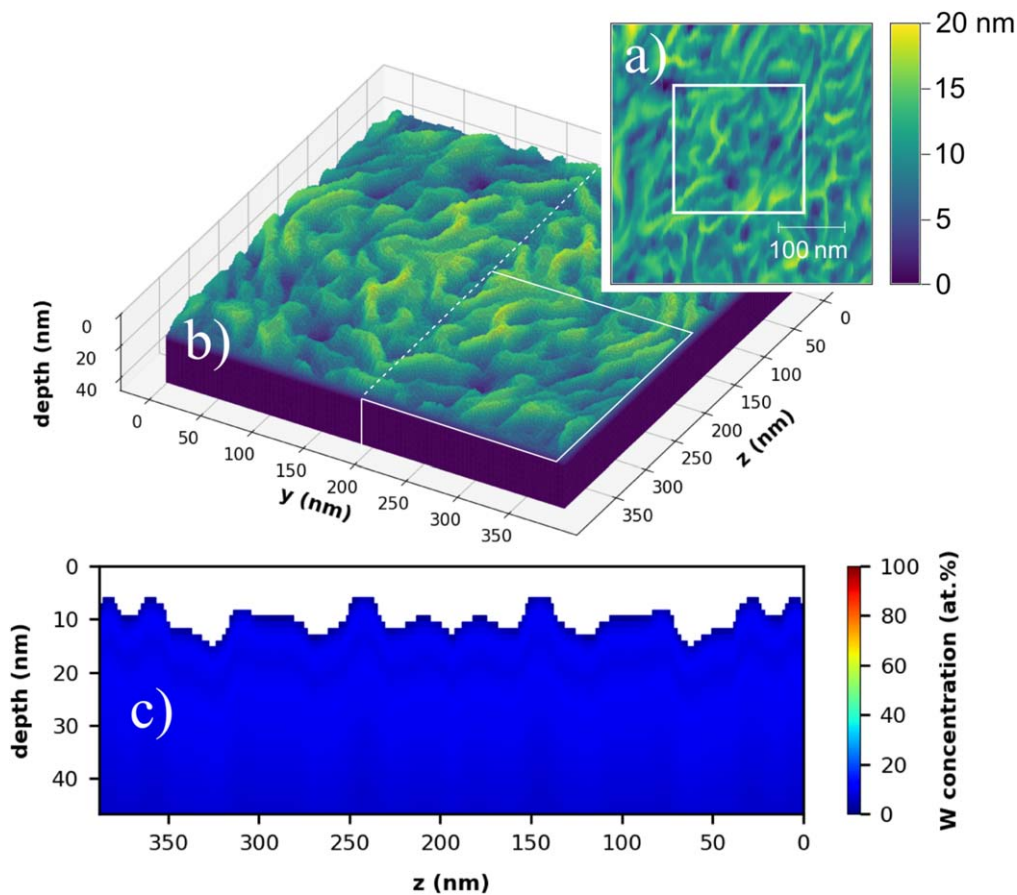
Figure 2. (a) An AFM image [12] measured on the unirradiated Fe-W sample served as the surface morphology input for our TRI3DYN simulations. For computational reasons, height information was extracted from only a part of the image (indicated by the white square). To ensure periodic boundary conditions, this image had to be mirrored in both lateral directions, resulting in the voxel layer data shown in (b). There, every voxel has a size of $11 \times 19 \times 19$ Å^3 (depth $\times$ y $\times$ z). The colour code in (a) and (b) is equivalent. In (c) a cross-section through the middle of the voxel layer data (white dashed line in (b)) can be seen, showing the initial W concentration according to sputter-XPS measurements.

projectiles, each representing a certain number of real projectiles. A higher statistical accuracy can be achieved with a high pseudoatom number, but at the cost of computation time. In the simulations shown here a pseudoatom to real atom factor of 17.1 was used to ensure high accuracy, leading to a total computation time of about 1300 CPU hours.

Figure 2(a) shows the experimentally obtained AFM image from [12]. The marked white square in figure 2(a) with a lateral expansion of 194×194 nm^2 was used as topography input for TRI3DYN. To fulfill the necessary periodic boundary conditions, this image had to be mirrored in both lateral directions. Since the original surface morphology has no particular preferred orientation, no information is lost. The resulting initial root-mean-square-roughness (RMSR) is 2.9 nm, i.e., almost the same as the full-sized AFM image (3.2 nm). The initial elemental depth profile input for TRI3-DYN was taken from either the sputter-XPS (figure 1) or RBS (table 1). Due to the significant difference of these measurements, simulations were performed using input data from both techniques and the results were later compared to those of the experiments. The resulting (initial) voxel pile can be seen in figure 2(b), where only the first 40 voxel layers are displayed. As soon as a complete voxel layer is sputtered

away in the simulation, a new layer with the elemental distribution of the initial bottom layer is added at the bottom of the voxel pile. This should ensure that no projectile is transmitted through the bottom. Figure 2(c) shows a cross-section of the voxel pile, displaying the initial surface line structure and elemental W concentration.

3. Comparison of TRI3DYN simulations to experimental data

We started the comparison with experimental QCM data obtained for D projectiles at 250 eV impacting under an angle of incidence of 45°. A continuous drop in the mass removal rate with increasing fluence and at constant impinging ion flux was found. As can be seen in figure 3 (solid line), the mass removal rate starts at 1.1 amu/D and continuously drops to 0.5 amu/D after a total fluence of 4×10^{23} m^{-2} without any sign of reaching a steady state value. The standard interpretation of this behaviour in our previous work [12] and the work of other groups [10, 11, 16] is that due to preferential sputtering of Fe, the surface is enriched with W, thus reducing the sputtering yield considerably. Our simulations
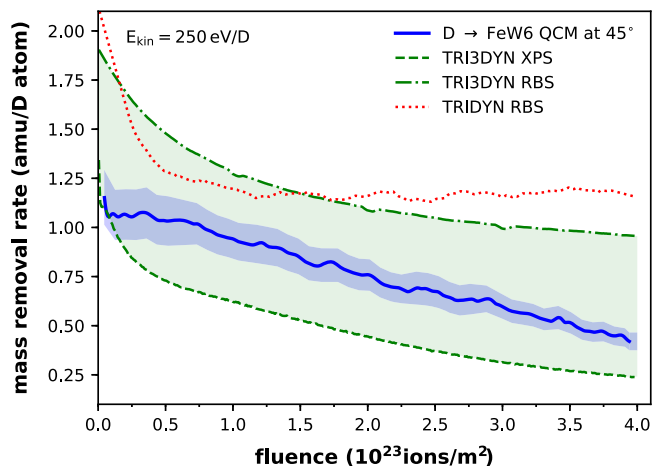
Figure 3. Fluence dependence of the mass removal rate under D ion bombardment at 250 eV/D and under 45°. The dashed and the dashed-dotted lines show TRI3DYN results, using RBS information and sputter-XPS data as input. The full line represents experimental results evaluated with the QCM technique and lies between the two TRI3DYN calculations. A clear decrease of the mass removal rate is observable, which is confirmed by TRI3DYN. A 1D simulation with TRIDYN shows a strong decrease of the mass removal rate and reaches steady state conditions after 1×10^{23} m^{-2}.

with TRI3DYN confirm this continuous reduction in the mass removal rate.

The TRI3DYN calculation using the XPS elemental depth data as input shows a quick drop from 1.25 amu/D to 0.75 amu/D after a fluence of only 5×10^{22} m^{-2}, followed by a slower decrease of the mass removal rate. Here the gradient of the mass removal rate shows a slope nearly identical to that of the QCM experiment. These calculations, however, slightly underestimate the measured mass removal. The TRI3DYN calculation using the RBS elemental depth data as input displays a generally higher mass removal rate, as compared to the QCM experiment. At low fluences, a higher gradient can be seen, which continuously decreases and does not reach a steady state even after a fluence of 4×10^{23} m^{-2}. The resulting mass removal rate is, however, larger by a factor of about 2 than the measured value. To test the influence of changes in the surface morphology, a simulation with TRIDYN (1D) (which uses RBS elemental depth information and a perfectly flat surface) is shown in figure 3 for comparison. The resulting mass removal rate is overestimated by TRIDYN as well (probably due to the use of the RBS input data). However, while a quick reduction of the mass removal rate is observable, steady state conditions are reached at about 1×10^{23} m^{-2}.

The assumed surface enrichment of W due to preferential sputtering of Fe [10–12] is confirmed by TRI3DYN. Figure 4 displays the calculated fluence dependence of the elemental surface concentration. Using the RBS data as input (figure 4(b)), a continuous Fe reduction and a W surface enrichment of up to 33% is calculated. With the XPS data (figure 4(a)) case, a quick depletion of the impurity layers containing O and C can be seen, thus exposing the underlying Fe and W layers. With increasing fluence, however, in this case the W enrichment at the surface reaches 76%. Unsurprisingly, these changes in elemental concentrations have a

direct effect on the sputtering yield, as can be seen by comparing figure 4 with figure 3. The increased mass removal rate at low fluences correlate with the low surface enrichment of W. Figure 4 also illustrates the modelled surface recession, which in the XPS case reaches about 47 nm and in the RBS case about 91 nm. The QCM experiments revealed a surface recession of 75 nm, which is in between. This value was also found in *post mortem* RBS measurements. A W surface enrichment of 30% when averaged over a depth of 1.2 nm was revealed by RBS.

The fact that TRIDYN (1D) is unable to reproduce the continuous decrease in the mass removal rate indicates that there might be a severe influence due to changes in surface morphology. In figure 5 we therefore compare the resulting surface morphology after a total fluence of 4×10^{23} m^{-2}. The measured AFM image in figure 5(a) shows quasi-periodically arranged nanodots, elongated slightly in the direction of the incoming ion beam [12]. The results of the TRI3DYN simulation figure 5(b) are strikingly similar, also showing quasi-periodically arranged nanodots of similar size, regardless of whether XPS or RBS data was used. As for the evolving surface roughness, an increase can be seen in both cases, slightly stronger in the RBS case. In the AFM measurements an increase in surface roughness from 3.2 nm to 6.4 nm RMSR is observed [12], while the TRI3DYN calculation shows a very similar increase of RMSR, from 2.9 nm to 5.3 nm.

4. Discussion

Figures 3 and 4 clearly demonstrate the necessity of precise elemental depth information in order to allow TRI3DYN to accurately predict absolute sputtering yields as a function of ion fluence. The drawbacks of RBS measurements are the lack of sensitivity to masses with low Z, such as O and C, and the limited depth resolution. Sputter-XPS on the other hand is a very surface-sensitive technique. However, since sputtering with Ar ions is used for depth profiling, this might lead to changes of the sample by the measurement. Therefore, the W concentrations in the sputter-XPS results in figure 1 are likely to be somewhat overestimated due to preferential sputtering (and consequently, Fe concentrations are underestimated). The true elemental composition is probably in between the two measurements, as suggested by figure 3. It is interesting that TRI3DYN is actually able to reproduce the surface pattern from the AFM image quite well, as can be seen by comparing figure 5(a) with 5(b). Figure 5(c) gives a cross-cut of the resulting voxel pile, revealing the local W concentration. The W concentration peaks on the elevations, preventing further erosion. In the valleys the W concentration is lower because of re-deposition of sputtered Fe. A closer look at the W concentration at the surface reveals an increased concentration in the +z direction, simply because this is the ion beam facing side. The effect of the shadowing of recessed areas can also be observed. The fact that TRI3DYN does not consider diffusion indicates that this effect plays no role at these temperatures. In the supplementary material (online version) stacks.iop.org/PSTOP/T171/014021/mmedia, we
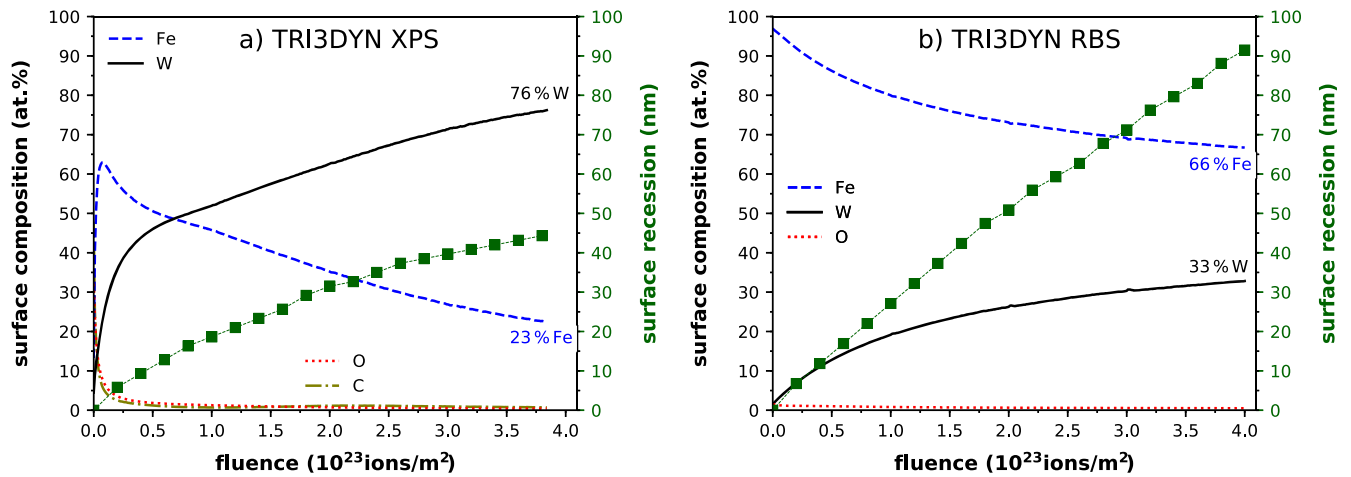
Figure 4. Fluence dependence of the elemental surface concentration and surface recession, evaluated with TRI3DYN. Using XPS data as input (a), a rapid depletion of impurities of O and C is followed by a steady increase of W surface concentration (thick black line). Higher fluences show a W surface enrichment of up to 76%. Using RBS elemental input data (b), the surface enrichment of W reaches 33%. In both cases the surface recession (square symbols) increases and slows down at higher fluences, due to W surface enrichment.
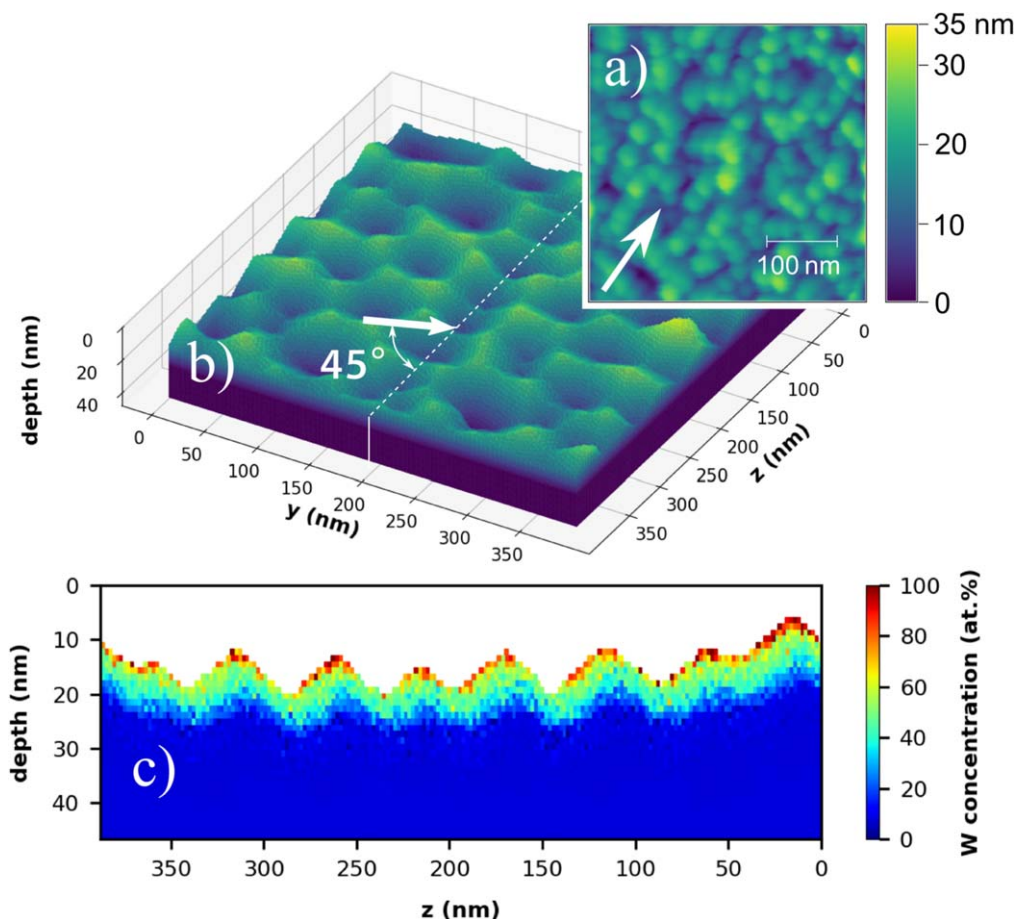
Figure 5. Surface morphology after a total D fluence of 4×10^{23} m^{-2} for 250 eV and under a 45° angle of incidence. The white arrows indicate the direction of the incident ion beam. In (a) the experimental AFM image (taken from [12]) of an irradiated sample is shown, while (b) displays the corresponding computational result of TRI3DYN, using XPS data as input. The colour code in (a) and (b) is equivalent. (c) is a cross-section through the middle of of the TRI3DYN voxel layer data (white dashed line in (b)), showing the resulting W enrichment at the surface, which acts as a protective layer.

present a fluence-dependent animation of the TRI3DYN simulation results, which demonstrates the dynamic development of the surface nanostructures, surface recession, and local W enrichment due to prolonged D irradiation.

5. Conclusion and outlook

The TU Wien QCM technique is a powerful way to investigate the dynamics of sputtering processes with high precision. It allows us to benchmark 3D MC-BCA codes such as TRI3DYN or SDTrimSP-3D. In this contribution we focus on comparison with TRI3DYN. As a test case we take Fe-W model films, sputtered with a D ion beam at 250 eV impact energy under an angle of incidence of 45°. We demonstrate that by including initial information about the surface morphology of the sample in combination with precise elemental depth profiles, TRI3DYN is capable of forecasting the outcome of experiments. Modification of the surface morphology during sputtering is clearly reflected in the sputtering behaviour, which cannot be modelled with a one-dimensional BCA code such as TRIDYN. Instead, TRI3DYN can reproduce the experimentally observed surface morphology changes, including the increase in surface roughness. Surprisingly, even rather low initial (RMS) roughnesses in the nm range have a significant influence on the sputtering behaviour. The possibility to use a voxel pile as input for a realistic surface will in future also allow us to simulate the sputtering of more complex nanostructures, such as W-fuzz [17]. The huge compuation time, however, limits these simulations to areas with rather small lateral extensions. Temperature-related effects such as diffusion can also severely influence the sputtering behaviour and surface relaxation processes, which are not yet included in TRI3DYN [18]. Although still under development, SDTrimSP-3D could be a promising alternative, since it also uses the voxel principle but is already parallelized, thus allowing faster computation [9].

ORCID iDs

R Stadlmayr ⬛ https://orcid.org/0000-0001-5194-1933
P S Szabo ⬛ https://orcid.org/0000-0002-7478-7999
F Aumayr ⬛ https://orcid.org/0000-0002-9788-0934

References

[1] Behrisch R *et al* 2007 *Sputtering by Particle Bombardment* (*Top. Appl. Phys.* vol 110) (Berlin Heidelberg: Springer) (https://doi.org/10.1007/978-3-540-44502-9)
[2] Williams P 1979 *Surf. Sci.* **90** 588
[3] Kelly P J *et al* 2000 *Vacuum* **56** 159
[4] Szabo P S *et al* 2018 *Icarus* **314** 98
[5] Brezinsek S *et al* 2017 *Nucl. Fusion* **57** 116041
[6] Pitts R A *et al* 2011 *J. Nucl. Mater.* **415** S957
[7] Hayderer G *et al* 1999 *Rev. Sci. Instrum.* **70** 3696
[8] Möller W 2014 *Nucl. Instrum. Methods Phys. Res., Sect. B* **322** 23
[9] Von Toussaint U *et al* 2017 *Phys. Scr.* T **170** 014056
[10] Roth J *et al* 2014 *J. Nucl. Mater.* **454** 1
[11] Lindau R *et al* 2005 *Fusion Eng. Des.* **75–79** 989
[12] Berger B M *et al* 2017 *Nuclear Materials and Energy* **12** 468
[13] Möller W *et al* 1984 *Nucl. Instrum. Methods Phys. Res., Sect. B* **2** 814
[14] Mutzke A *et al* 2013 Sdtrimsp-2d: Simulation of particles bombarding on a two-dimensional target – version 2.0 *Report, Max-Planck-Institut für Plasmaphysik*
[15] Stadlmayr R *et al* 2018 *Nucl. Instrum. Methods Phys. Res., Sect. B* **430** 42
[16] Sugiyama K *et al* 2015 *J. Nucl. Mater.* **463** 272
[17] Shin K *et al* 2009 *Nucl. Fusion* **49** 095005
[18] Koslowski H R *et al* 2018 *Nuclear Materials and Energy* **16** 181